ACS OMEGA

http://pubs.acs.org/journal/acsodf

Article

Evolution Characteristics of the Microstructure with Different Fracturing Fluids: An Experimental Study of Guizhou Bituminous Coal

Liangwei Li,* Haitao Sun, Wenbin Wu, Shaojie Zuo,* and Peng Sun

Cite This: *ACS Omega* 2023, 8, 29803−29811

Read Online

ACCESS | Metrics & More | Article Recommendations

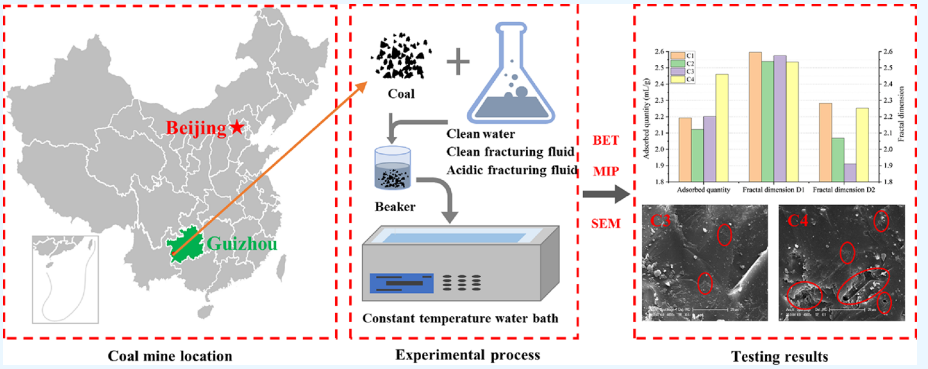

ABSTRACT: Fracturing fluid is a key factor affecting the hydraulic fracture morphology and coal microstructure, which plays a key role in the hydraulic fracturing effect. To compare the effect of clean water, clean fracturing fluid, and acid fracturing fluid on the pore structure of coal, this paper used high-pressure mercury injection (MIP), low-temperature N_2 adsorption (LT-N_2A), and scanning electron microscopy (SEM) to determine the pore structure of Guizhou bituminous coal before and after the action of fracturing fluid. The results show that clean water can cause mineral expansion and reduce pore volume by about 6% and clean fracturing fluid and acid fracturing fluid can increase pore volume by 3 and 12%, respectively, due to different degrees of acidity. The MIP data show that the pore structure of coal samples is more complex after the action of different fracturing fluids, and acidic fracturing fluids can increase the fractal dimension of the pore by about 7%. The LT-N_2A data showed that the fractal dimension of micropores and transition pores decreased after the action of different fracturing fluids. In general, acid fracturing fluid has the best effect on the coal microstructure, followed by clean fracturing fluid, and the least effect on clean water.

1. INTRODUCTION

Affected by the shortage of fossil energy and the greenhouse effect, all countries in the world are actively exploring new energy.[1,2] Coalbed methane is a new type of clean energy with broad application prospects, which has attracted the attention of governments all over the world.[3,4] According to the data of the International Energy Agency (IEA), the total global coalbed methane resources buried at a depth of less than 2000 m can reach 260 trillion m^3, which is more than twice the proven reserves of conventional natural gas.[5] However, the coal seams are less permeable and need to be hydraulically fractured to increase the permeability before the drainage of coalbed methane, especially in China.[6,7] Fracturing fluid is a key factor affecting the hydraulic fracture morphology and coal microstructure and plays an important role in the process of hydraulic fracturing.[8−10]

At present, the fracturing fluids used in coal seam hydraulic fracturing mainly include water, active water, clean fracturing fluid, acidic fracturing fluid, foam fracturing fluid, supercritical CO_2, etc. Many scholars have also optimized the composition and proportion of fracturing fluid according to the characteristics of different coal grades. For example, Yang et al.[11] determined the composition and ratio of viscoelastic surfactant fracturing fluid by analyzing the rheological parameters of fracturing fluid and found that the permeability of coal seam could be increased by 178% compared with pure water. Pan et al.[12] proposed adding an anion dispersant to the fracturing fluid to reduce the likelihood of coal powder plugging hydraulic fractures, thereby improving the efficiency of coalbed

Received: June 19, 2023
Accepted: July 20, 2023
Published: August 1, 2023

methane extraction. Ju et al.[13] developed a foam fracturing fluid using hydroxypropyl guar as a stabilizer and analyzed the viscosity and foam stability of the fracturing fluid. Xu et al.[14] used self-synthesized thickener-quaternary polymer to prepare polymer fracturing fluid and found that after the action, the gas-friendly ability of coal can be reduced and the hydrophilic ability of coal can be improved. Wang et al.[15] optimized the anionic fracturing fluid through viscosity, shear resistance, residue, etc., and found that compared with clean water, anionic clean fracturing fluid can increase the gas permeability of coal seams by up to 131%. Wang et al.[16] optimized the proportion of clean fracturing fluid with a cationic viscoelastic surfactant as the main component, which can greatly improve the viscosity, wettability, and shear stability of fracturing fluid on coal. Wang et al.[17] used a bisamido cationic surfactant to prepare a new clean fracturing fluid and determined the advantages of the fracturing fluid in terms of viscosity and fluid loss. In general, many scholars have optimized fracturing fluids from different angles, enhanced the effect of fracturing fluids, and made certain contributions to the development of fracturing fluids.

For the effect of fracturing fluid on the physical structure of coal seam, scholars mainly analyzed the effect of fracturing fluid on the morphology of hydraulic fractures and the pore structure of coal. Li et al.[18] found that fracturing fluid can not only change the micropore structure of coal but also enhance the mechanical sensitivity of coal and reduce the mechanical strength of coal. Yang et al.[19] used water, liquid CO_2, and supercritical CO_2 for fracturing and found that supercritical CO_2 had the lowest fracture initiation pressure and produced the largest number and roughness of hydraulic fractures. Lu et al.[20] analyzed the pore structure of coal after fracturing fluid action at different temperatures through fractal theory and found that a lower temperature than 323.15 K is more conducive to vigorously reform the pore structure of coal. Zuo et al.[21] compared the effect of clean fracturing fluid on the pore structure and adsorption capacity of coal samples of different coal ranks and found that clean fracturing fluid is more suitable for coal seams with middle and high-rank metamorphism. Xue et al.[22] studied the change in pore structure of coal after the action of different clean fracturing fluids and found that water-based fracturing fluids may affect pore shape and fractal dimension through residues but have no great influence on the chemical structure. Huang et al.[23] studied the pore structure of coal samples after the action of VES-based fracturing fluid and believed that fracturing fluid entered and adhered to coal pores to change the pore structure of coal. Zhou et al.[24] studied the effect of guar-based fracturing fluid and C-VES clean fracturing fluid on the coal microstructure and found that C-VES clean fracturing fluid can significantly affect the functional groups and wettability of coal. Huang et al.[25] found that guar-based fracturing fluid did not have a large impact on the functional group structure of coal, but the presence of hydroxypropyl guar hindered the diffusion and migration of gas. These scholars analyzed the effect of different fracturing fluids on the modification of the coal pore structure and confirmed the effect of fracturing fluid on the modification of the coal microstructure.

In summary, it can be found that these studies are mainly aimed at the effect of one fracturing fluid, and there are few comparative analyses of the effects of different fracturing fluids. Therefore, this paper studies the effect of different fracturing fluids on the pore structure of bituminous coal and analyzes the pore structure of coal samples by MIP, LT-N_2A, and SEM. The research results can provide a certain reference value for the development of coalbed methane.

2. EXPERIMENTAL DESIGN

2.1. Preparation of the Coal Sample. The coal used in the experiments came from the Shanjiaoshu Coal Mine in Panjiang mining area in Guizhou Province, China. The gas pressure and gas content of Shanjiaoshu Coal Mine are 0.79 MPa and 8.6 m^3/t, respectively. A large lump of coal sample was broken and processed into particles with the size of 0.2−0.3 mm as the experimental samples. The coal sample was confirmed as bituminous coal by industrial analysis, and the specific results are shown in Table 1.

Table 1. Specific Results of Industrial Analysis

M_{ad}/%	A_{ad}/%	V_{daf}/%	FC_{ad}/%
2.07	11.95	19.41	66.57

2.2. Experimental Process. The fracturing fluids used in the experiment are the three most commonly used fracturing fluids, namely, clean water, clean fracturing fluid, and acidic fracturing fluid. The raw coal is numbered C1, and the coals treated with clean water, clean fracturing fluid, and acid fracturing fluid are numbered C2, C3, and C4, respectively. Clean water is the lowest-cost fracturing fluid and is less effective. Clean fracturing fluid has the advantages of small filtration loss, no residue, and little damage to the reservoir, but the cost is relatively high. Acid fracturing fluid has a good effect on the modification of the pore structure but has the disadvantages of damaging the reservoir and poor thickening ability. All of the fracturing fluids were composed of distilled water. The clean water is distilled water. The composition and ratio of clean water fracturing fluid are 0.8 wt % CTAC + 0.2 wt % Nasal + 1 wt % KCl. The composition and ratio of the acidic fracturing fluid are 0.5 wt % HCl + 0.5 wt % CTAB.[26,27]

The coal sample and fracturing fluid were placed in a beaker and covered with plastic wrap, as shown in Figure 1. The beaker was then placed in a thermostatic water bath at 30 °C for 12 h. After that, the coal sample was filtered out of the fracturing fluid and cleaned with distilled water. Finally, the cleaned coal samples were dried at 70 °C for 24 h.

2.3. Measurement Means. To more accurately and intuitively understand the changes in the pore structure of coal samples, three testing methods, MIP, LT-N_2A, and SEM, are used here. MIP is to obtain the volume and number of pores by pressing mercury into the pores of coal at high pressure and can only obtain the results of pores larger than 5 nm. LT-N_2A obtains the distribution of pore volume and pore size by analyzing the adsorption amount of N_2 in the micropores of coal samples under different relative pressures, but it can only measure the pores in the range of 2−200 nm. SEM can directly obtain the morphology and distribution of pores on the surface of coal samples, which is a supplement to the experimental results of MIP and LT-N_2A.

2.3.1. MIP Tests. A high-performance automated mercury injection instrument (AutoPore IV 9500, USA) was used for analysis. The maximum injection pressure is 228 MPa.

2.3.2. LT-N_2A Tests. N_2 adsorption/desorption was performed using a high-performance specific surface and porosity analyzer (ASAP 2460, USA). First, the coal samples were vacuumed for 12 h, and then nitrogen adsorption and

https://doi.org/10.1021/acsomega.3c04351
ACS Omega 2023, 8, 29803−29811

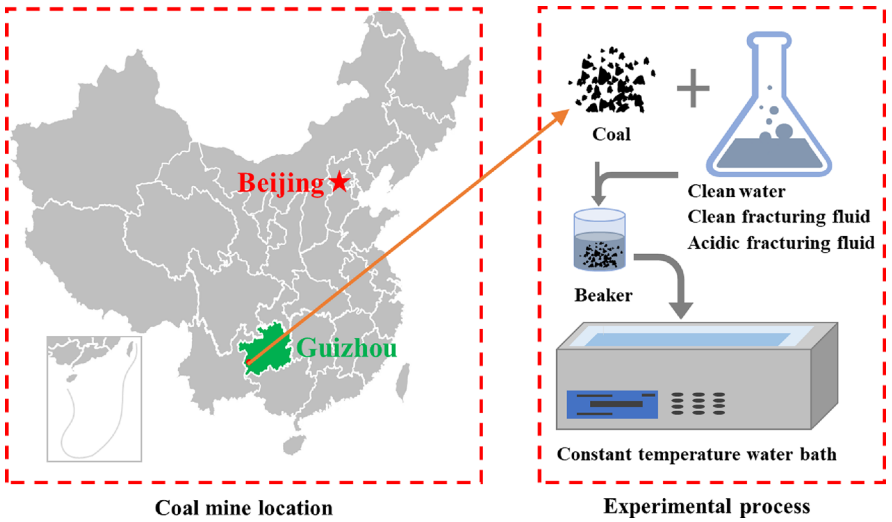

Figure 1. Diagram of experimental flow.

desorption experiments were carried out under relative pressure ($0.001 < P/P_0 < 0.995$).

2.3.3. SEM Tests. Scanning electron microscopy (COXEM EM30, Korea) was used to observe the coal surface before and after treatment with different fracturing fluids. Before the test, the coal needs to be dried and sprayed with gold powder on the coal surface.

3. RESULTS AND DISCUSSION

3.1. MIP Tests. The intrusion and extrusion mercury curves of the four coal samples are shown in Figure 2. Affected by the

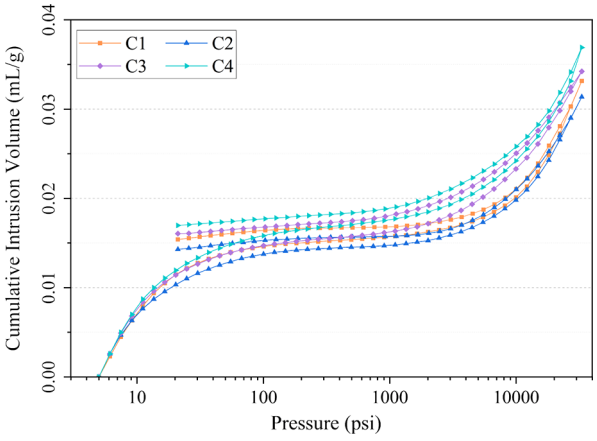

Figure 2. Intrusion−extrusion mercury curves.

basic pore structure of the raw coal samples, the mercury intrusion and extrusion curves of the coal samples treated with different fracturing fluids are basically similar, with little difference. The initial stage of growth is fast, the middle stage of growth is slow, and the end stage of growth is fast. The total pore volume of raw coal is 0.331 mL/g, and the total pore volumes of C2, C3, and C4 coal samples are 0.314, 0.342, and 0.369 mL/g, respectively. The pore volume of C2 decreased by about 5%, which should be due to the expansion of clay minerals after the action of distilled water, resulting in a decrease in the total pore volume. The pore volumes of C3 and C4 increased by about 3 and 11%, respectively, mainly due to the chemical reaction between H+ (produced by fracturing fluid) and minerals in coal, which increased the total pore volume. Since the H+ concentration of the acidic fracturing fluid (pH is 0.86) is higher than that of the clean fracturing fluid (pH is 6.72), the acidic fracturing fluid has a better modification effect on coal pore volume. In addition, the pore size distribution curves of coal samples after different coal samples were also drawn, as shown in Figure 3. To facilitate

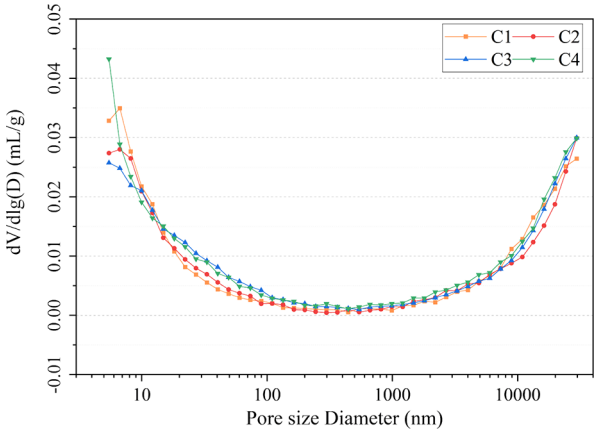

Figure 3. Pore volume change with different pore size diameters.

data analysis, according to the pore size classification scheme developed by the Soviet scholar Hodot, the pores in coal rocks are divided into four categories: micropores ($d < 10$ nm), transition pores ($10 < d < 100$ nm), mesopores (100 nm $< d <$ 1000 nm), and macropores ($d > 1000$ nm). It can be found that the pores of the coal sample are mainly micropores and macropores, with fewer transition pores and the least mesopores. For the pore size distribution curve, the transition pores of the coal samples changed significantly after different fracturing fluids, and the micropores also had some changes, while the changes of the mesopores and macropores were not obvious.[28]

To understand the variation of pores with different pore sizes more intuitively, a histogram of pore volume and pore surface area of different sizes was drawn (Figures 4 and 5). For C2, the pores of different pore sizes all decrease, indicating that the clay minerals around the pores will expand when exposed

https://doi.org/10.1021/acsomega.3c04351
ACS Omega 2023, 8, 29803−29811

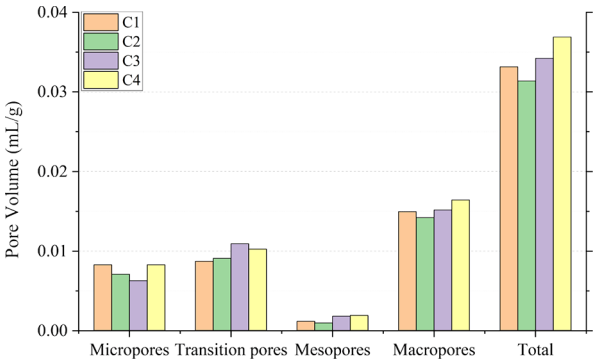

Figure 4. Pore volume of different pore categories.

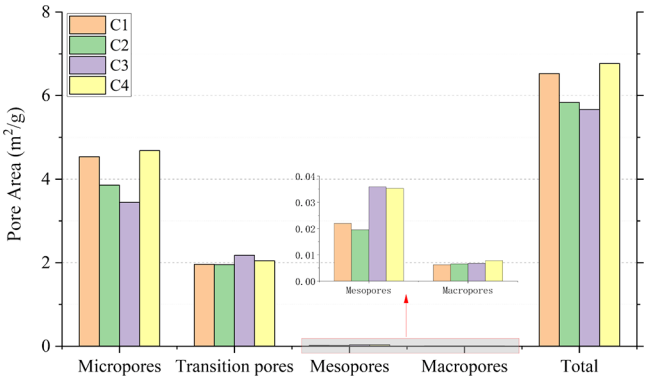

Figure 5. Pore area of different pore categories.

to water. The pore volume of the micropores of C3 decreased, while the pore volume of the transition pores and mesopores increased significantly, and the pore volume of the macropores did not change much. The main reason is that after the clean fracturing fluid reacts with minerals, the pore size will increase and the number of micropores will decrease. In addition, clean fracturing fluid has a limited effect on pore size modification, and the size range of micropores and transition pores in pore size classification is small, which makes the volume of micropores and transition pores more likely to change. The acidic fracturing fluid reacts better with the minerals, creating some new pores in the coal. Therefore, micropores did not change much in C4, but transition pores, mesopores, and macropores all increased.

For the pore surface area (Figure 5), it can be found that there are mainly micropores and transition pores. This is mainly due to the nature of the specific surface area. For the same volume, the smaller the pore size, the larger the total surface area. The total surface area of distilled water and clean fracturing fluid both decreased but remained basically unchanged after acidic fracturing fluid is applied. The main reason is that after the action of distilled water, the swelling of the clay leads to the closure of some pore micropores, thereby reducing the surface area of the micropores. The clean fracturing fluid increases the overall pore size, thereby reducing the total pore surface area. After the acidic fracturing fluid acts, some new micropores are produced so that the pore surface area of the micropores basically remains unchanged. The size of the transition pores increases but the number increases, and the surface area does not change much.

To further analyze the pore structure of coal, the fractal dimension of the permeable pores of coal is calculated. The larger the fractal dimension, the more complex the pore structure. Here, the Washburn equation is used to establish the double-logarithmic regression equation of pressure and mercury injection to calculate the fractal dimension D, as shown in eq 1.

$$\ln(d_V/d_P) \propto (D-4)\lg P \tag{1}$$

where P is the pressure (MPa), V is the corresponding mercury injection volume (mL), and D is the fractal dimension.

Assuming that the slope of the fitting curve is k, the fractal dimension is $k + 4$. Generally speaking, the fractal dimension number is between 2 and 3. When the fractal dimension is too large or too small, it cannot be used to analyze the fractal characteristics of three-dimensional porous media.

Because coal is compressible, when the mercury injection pressure is too high, the coal matrix will produce compression deformation and pore destruction, which will make the experimental results inaccurate. We analyzed Figure 6 and found that when P = 400 psi ($\ln P = 2.6$), the two sides of the point showed different trends. Therefore, we can use P = 400 psi as the cut-off point to carry out piecewise fitting, as shown in Figure 6. At the same time, it can be found that when the pressure is greater than 400 psi, the fractal dimension obtained by calculation is greater than 3, so the fractal dimension of this stage is not considered.[29] Effective fractal dimension calculation results are shown in Table 2.

To more intuitively compare the effects of different fracturing fluids on the pore structure modification of coal, we put the relevant parameters obtained by the MIP into Table 2. In addition to the total pore volume and pore surface area, we also compared average pore size, fractal dimension, tortuosity, and permeability. The average pore size reflects the coal sample's gas adsorption capacity and gas flow capacity to a certain extent. The larger the pore size, the more favorable the gas flow. The tortuosity depends on the tortuosity of the pores and fissures. The greater the tortuosity, the greater the gas flow resistance and the more difficult the flow. It can be found that the average pore diameter of coal becomes larger after the fracturing fluid is applied, and the clean fracturing fluid has the best effect on pore diameter modification. In fact, according to experience and data of pore volume changes, it can be seen that acidic fracturing fluid has the best effect on the modification of the coal microstructure. However, affected by the new micropores produced by the acidic fracturing fluid, the estimated pore size does not change much after the acidic fracturing fluid is applied. In addition, the fractal dimension is the largest after the acidic fracturing fluid acts, that is, the pore structure is more developed, which proves the effect of the acidic fracturing fluid on coal. The tortuosity is mainly used to measure the resistance of the seepage channel, and the smaller the tortuosity, the smaller the flow resistance. The tortuosity of the coal samples decreased after the action of different fracturing fluids, and the tortuosity was the smallest after the action of the clean fracturing fluid. The permeability of coal increases after fracturing fluid is applied, and clean fracturing fluid has the greatest impact on permeability. According to the conventional understanding and the change of pore volume parameters, we can probably know that acidic fracturing fluid has the best effect on the transformation of coal, that is, the increase in pore volume is the largest. However, we also found that the permeability data did not support this conclusion, and there was a deviation from the conclusions of others.[30] Therefore, we believe that the permeability data obtained from the mercury injection experiment are not reliable and cannot

https://doi.org/10.1021/acsomega.3c04351
ACS Omega 2023, 8, 29803−29811

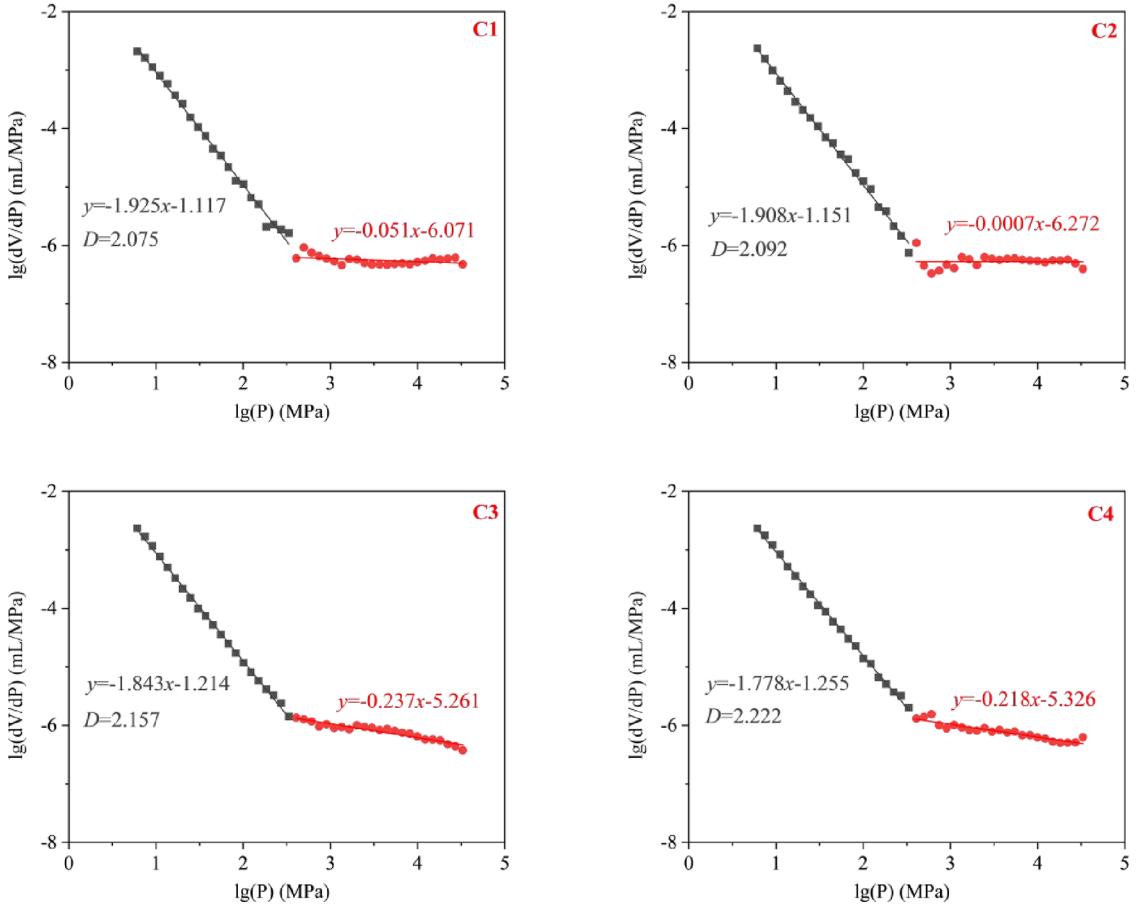

Figure 6. Effective fractal dimension of MIP tests.

Table 2. Calculation Results of the Basic Parameters

sample	total volume (mL/g)	pore area (m^2/g)	average pore size (nm)	fractal dimension	tortuosity	permeability (mD)
C1	0.033	6.526	20.320	2.075	23.251	4.787
C2	0.031	5.835	20.509	2.092	20.751	5.364
C3	0.034	5.667	24.156	2.157	16.452	6.765
C4	0.037	6.774	21.787	2.222	20.224	5.503

be used to evaluate coal samples. The main reason is that the porosity obtained by MIP is calculated according to the micropore structure parameters of granular coal, and relevant theories are shown in eq 2. It can be found that the parameter of average pore size is taken into account in the calculation process. However, the average pore diameter of acid fracturing fluid decreases due to the production of more micropores, thus reducing the permeability of the coal sample. In fact, the permeability of coal samples will increase to some extent due to the reconstruction of original pores after the action of acid fracturing fluid. In addition, coal has a dual structure of pores and fissures. The coal samples used in the MIP tests were coal particles of 0.2−0.3 mm, which did not take into account the key factors affecting the penetration effect such as natural joints, natural fractures, and artificial fractures of coal. Therefore, the results of MIP tests have a certain one-sidedness, which can be used to evaluate the pore structure of coal, but cannot completely show the permeability of coal.

$$K = \frac{\varphi}{8\tau} r^2 \quad (2)$$

where K is the permeability (mD), φ is the porosity, r is the average pore radius (nm), and τ is the tortuosity of the pores.

3.2. LT-N_2A Tests. To understand the distribution of smaller pores, we also performed liquid nitrogen adsorption experiments. The adsorption/desorption curves of coal samples after different fracturing fluids are basically similar, as shown in Figure 7. The maximum adsorption capacities of C1, C2, C3, and C4 were 2.19, 2.12, 2.20, and 2.46 mL/g, respectively. According to the adsorption/desorption curve, we can know that the pores of coal samples are mainly micropores, especially the pores with a pore size smaller than 5 nm. In the range of relative pressure less than 0.5, the adsorption curves and desorption curves of different coal samples are nearly coincident. The results show that there are mainly semi-open pores in the small pore-size section, which is conducive to gas desorption. It is worth mentioning that in the range of relative pressure greater than 0.5, C4 coal samples show abrupt changes in the N_2 desorption curve (the curve suddenly drops). C1, C2, and C3 coal samples also have abrupt changes here, but the decrease is not large, and it is more obvious in the coal samples after the action of acid fracturing fluid. This indicates that there are more or larger ink bottle-shaped pores

https://doi.org/10.1021/acsomega.3c04351
ACS Omega 2023, 8, 29803−29811

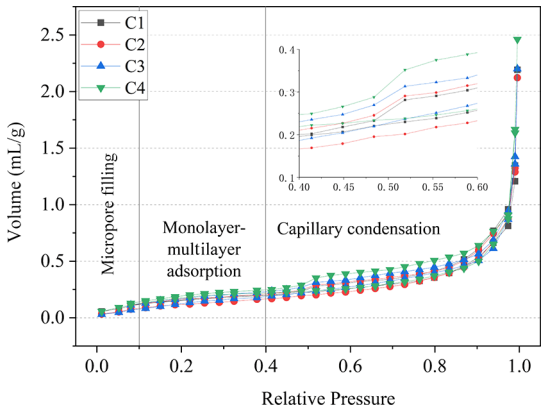

Figure 7. Adsorption/desorption curves of different coal samples.

in the coal samples after the action of acid fracturing fluid. In the process of relative pressure drop, N_2 in the large pores starts to desorb first, N_2 in the small-sized pores also begins to desorb gradually, and the desorption line gradually decreases. When the relative pressure drops to the inflection point, the condensate N_2 in the ink bottle-shaped pores will all gush out instantly, causing the desorption curve to drop rapidly. When the N_2 in the ink bottle-shaped pores is released, the desorption curve returns to the normal state and coincides with the adsorption curve. This is why there is an inflection point in the desorption curve.

Because the adsorption/desorption curve of liquid nitrogen has a sudden change when the relative pressure is 0.5, although the change is not large, for the accuracy of the calculation of the fractal results, we performed a segmented calculation when calculating the fractal dimension. That is to calculate the fractal dimension when the relative pressure is greater than 0.5 and less than 0.5, respectively.

In addition, the fractal dimension of the liquid nitrogen adsorption curve was analyzed. Here, the Frenkel−Halsey−Hill (FHH) model is used to calculate the fractal dimension D, as shown in eq 3.[31]

$$\ln(V/V_0) = C + A[\ln(\ln(P_0/P))] \quad (3)$$

where P_0 is the gas-saturated vapor pressure of N_2 (MPa), P is the actual pressure (MPa), V is the adsorption amount of N_2 corresponding to P (mL/g), V_0 is the monolayer volume of N_2 adsorption at standard temperature and pressure (mL/g), C is the constant, and A is the slope of the curve obtained by fitting. Then, the fractal dimension is $A + 3$.

Because the adsorption/desorption curve of liquid nitrogen had a sudden change when the relative pressure was 0.5, although the change was not significant, we carried out a segmented calculation when calculating the fractal dimension for the accuracy of the calculation of fractal results. That is, the fractal dimension is calculated separately for relative pressures greater than 0.5 and less than 0.5. The fractal dimension is generally between 2 and 3, and the closer to 2, the smoother the pores. The specific fitting curve is shown in Figure 8.

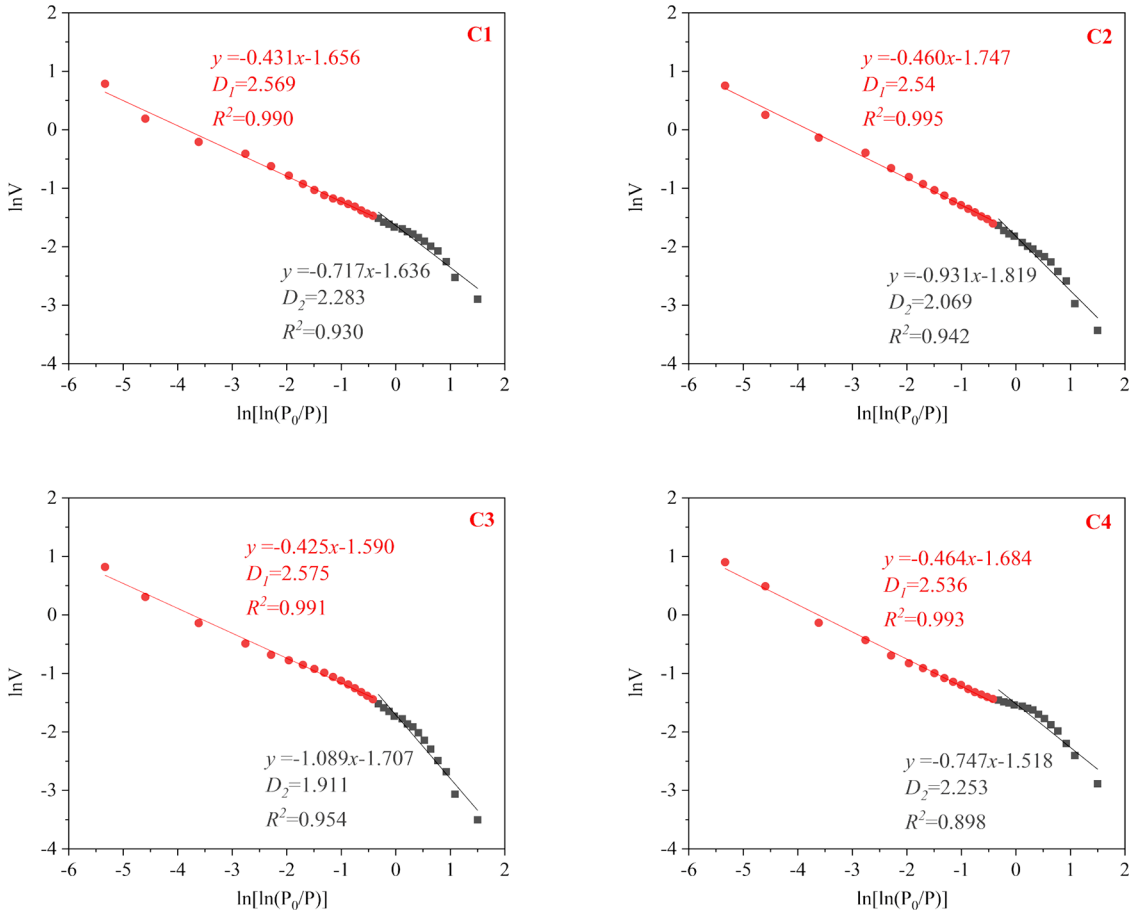

Figure 8. Fractal dimension of LT-N_2A tests.

https://doi.org/10.1021/acsomega.3c04351
ACS Omega 2023, 8, 29803−29811

To understand the accuracy of the LT-N_2A results, the micropore and transition pore data measured by the MIP experiment were compared, as shown in Figure 9. It can be

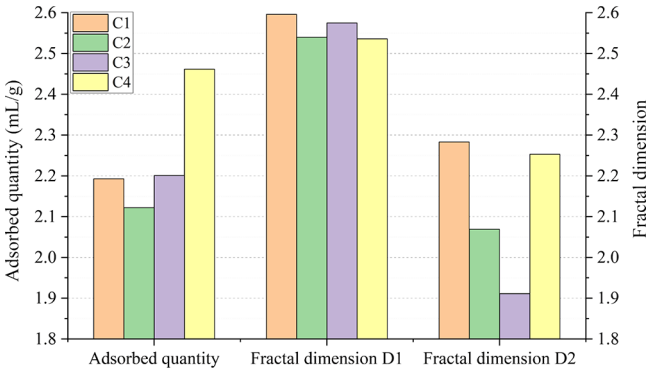

Figure 9. Adsorbed quantity and fractal dimension of different coal samples.

found that the pore volume of C2 treated with clean water is reduced by about 3%, and the pore volume of C3 treated with the clean fracturing fluid is basically unchanged, which is consistent with the MIP test data. However, the pore volume of C4 treated with acid fracturing fluid significantly increased by about 12%, which was more obvious than that of MIP test data. This supports the hypothesis that acid fracturing fluid generates new micropores in coal seams. It can also be found that the fractal dimension D_1 is significantly greater than the fractal dimension D_2, which means that the smaller the pores, the larger the fractal dimension. This means that the smaller the pore structure is, the more complex it is, which is more unfavorable to the flow of methane. In addition, the fractal dimension D_1 changes very little after the action of different fracturing fluids, which is only 1 or 2%. Then, the fractal dimension D_2 changes greatly. Compared with the raw coal sample (C1), C2, C3, and C4 are reduced by 10, 16, and 2%, respectively. The reason why the fractal dimension D_2 of the coal sample decreases after being treated with clean water should be the closure of some pores. The closure of these pores may reduce the connectivity of previously connected pores, thus reducing the fractal dimension. After the action of clean fracturing fluid, the original clay minerals in the pores will be dissolved, making the pore channel smoother, thus reducing the fractal dimension. However, new pores will be generated after the action of acid fracturing fluid, which will increase the degree of connectivity of pores. The combination of the two effects will make the fractal dimension change a little. There is a certain difference between the fractal dimension measured by liquid nitrogen and that measured by mercury injection, mainly because of the difference in the measured pore diameter range and measurement principle by mercury injection and liquid nitrogen. The pore size range of mercury injection was 5−340,000 nm, while the pore size range of liquid nitrogen was 2−500 nm. The pore targets of the two analyses are different, so there will be different trends of fractal dimension. The high pressure of mercury injection may cause damage to some pores, resulting in certain errors in the results. In addition, fracturing fluid (especially clean fracturing fluid) will have a great impact on the micropores and transition pores of coal, resulting in a great change in the pore volume and fractal dimension of micropores and transition pores.

3.3. SEM Tests. To observe the evolution of the pore structure of coal samples more intuitively, the coal samples were observed with an electron microscope. The SEM images of coal samples under different treatment conditions are shown in Figure 10. It can be found that there are more coal matrix

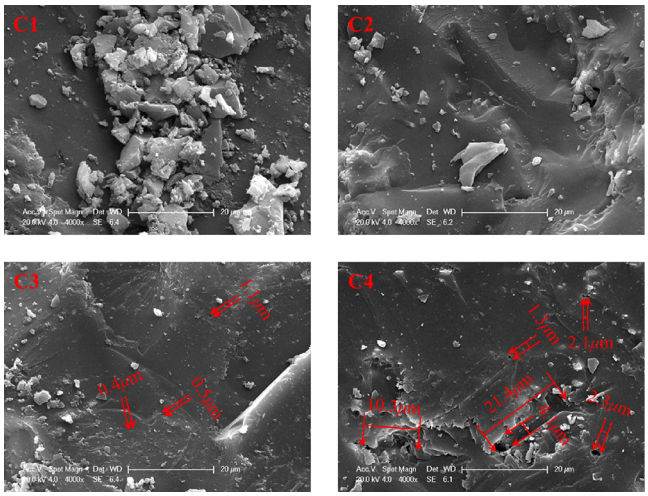

Figure 10. SEM images of different coal samples.

particles (attached minerals) on the surface of raw coal (C1), and the number of matrix particles (attached minerals) on the coal surface is significantly reduced after different fracturing fluid treatments. This is mainly due to the long-term interaction between coal and fracturing fluid, which leads to the dissolution of matrix particles (attached minerals) in the fracturing fluid. For raw coal (C1), these mineral particles are likely to clog pores and block gas flow channels. After the action of clean water (C2), the attached minerals on the coal surface will only be reduced. The main reason is that the mineral particles fall off during the process of immersing, washing, and stirring of the coal samples, rather than chemical reactions. This is also the reason why it is difficult to form new pores in the coal. After being treated with the clean fracturing fluid (C3), a small number of tiny pores were produced on the coal surface, as marked in Figure 10. This is because the fracturing fluid reacts with minerals, and the specific possible chemical reaction equations are eqs 4−10.[29,31] Due to the weak acidity of the clean fracturing fluid, the pores produced are small in number and size, mostly smaller than 1 μm. The acidic fracturing fluid is more acidic, more pores will be produced on the coal sample surface (C4) after the action, and the pore size is relatively large. In addition, under the action of acidic fracturing fluid, it will have a violent chemical reaction with coal, which will erode the coal and form grooves with a certain depth (the size is 4 μm × 21 μm). This is very beneficial to the flow and extraction of coal seam gas.

$$Fe_2O_3 + H^+ \rightarrow Fe^{3+} + H_2O \quad (4)$$

$$FeS_2 + H^+ \rightarrow Fe^{2+} + H_2S + S \quad (5)$$

$$CaCO_3 + H^+ \rightarrow Ca^{2+} + H_2O + CO_2 \quad (6)$$

$$CaMg(CO_3)_2 + H^+ \rightarrow Ca^{2+} + Mg^{2+} + H_2O + CO_2 \quad (7)$$

https://doi.org/10.1021/acsomega.3c04351
ACS Omega 2023, 8, 29803−29811

$$K_3Fe_4Si_4Al_7O_{20}(OH)_4 + H^+ \rightarrow Al^{3+} + K^+ + Fe^{2+} + Si^{4+} + H_2O \quad (8)$$

$$Al_2Si_2O_5(OH)_4 + H^+ \rightarrow Al^{3+} + Si^{4+} + H_2O \quad (9)$$

$$Si_6Al_4MgFe_3Na_4O_{20}(OH)_4 + H^+ \rightarrow Al^{3+} + Si^{4+} + Mg^{2+} + Fe^{2+} + Na^+ + H_2O \quad (10)$$

4. CONCLUSIONS

(1) There are certain differences in the changing trend of coal pore structure after the action of different fracturing fluids. The effect of clean water will lead to mineral expansion and reduce pore volume by about 6%, while clean fracturing fluid and acid fracturing fluid increase pore volume by 3 and 12%, respectively, due to the different degrees of acidity.

(2) The complexity of the micropore structure was evaluated by fractal dimension. According to MIP data, it is found that the fractal dimension of coal samples increases after the action of different fracturing fluids, and the pore structure is more complex. Acidic fracturing fluids can increase the fractal dimension of the pore by about 7%. LT-N_2A data mainly showed the changes in micropores and transition pores, and the fractal dimension of micropores and transition pores decreased after the action of different fracturing fluids.

(3) According to SEM images and pore volume variation amplitude, it can be seen that acid fracturing fluid has the best effect on coal modification, followed by clean fracturing fluid, and clean water has the least effect.

AUTHOR INFORMATION

Corresponding Authors

Liangwei Li − *School of Resources and Safety Engineering, Chongqing University, Chongqing 400044 Sichuan, China; China Coal Technology and Engineering Group Chongqing Research Institute, Chongqing 400039, China*; Email: sccqxu1@foxmail.com

Shaojie Zuo − *College of Mining, Guizhou University, Guiyang 550025, China; Guizhou Provincial Double Carbon and Renewable Energy Technology Innovation Research Institute, Guizhou University, Guiyang 550025, China*; orcid.org/0000-0002-3748-8340; Email: sjzuo@gzu.edu.cn

Authors

Haitao Sun − *School of Resources and Safety Engineering, Chongqing University, Chongqing 400044 Sichuan, China; China Coal Technology and Engineering Group Chongqing Research Institute, Chongqing 400039, China*

Wenbin Wu − *China Coal Technology and Engineering Group Chongqing Research Institute, Chongqing 400039, China; Shandong University of Science and Technology, Qingdao 266590, China*

Peng Sun − *School of Resources and Safety Engineering, Chongqing University, Chongqing 400044 Sichuan, China; China Coal Technology and Engineering Group Chongqing Research Institute, Chongqing 400039, China*

Complete contact information is available at: https://pubs.acs.org/10.1021/acsomega.3c04351

Notes

The authors declare no competing financial interest.

ACKNOWLEDGMENTS

The study was supported by Natural Science Foundation of Chongqing (cstc2021jcyj-msxmX0564), the Technological Innovation and Entrepreneurship Fund Special Project of Tiandi Technology Co., Ltd. (2022-2-TD-ZD008), Guizhou Provincial Science and Technology Projects (ZK[2022] general 163, Zhong Da Zhuan Xiang Zi [2021]3001, Zhi Cheng [2022] general 016), the open project of Guizhou Provincial Double Carbon and Renewable Energy Technology Innovation Research Institute (DCRE-2023-14), and the Talent Introduction Project of Guizhou University (Gui Da Ren Ji He Zi 2020-57).

REFERENCES

(1) Chen, R.; Bao, Y.; Zhang, Y. A Review of Biogenic Coalbed Methane Experimental Studies in China. *Microorganisms* **2023**, *11*, 304.

(2) Tao, S.; Chen, S.; Pan, Z. Current status, challenges, and policy suggestions for coalbed methane industry development in China: A review. *Energy Sci. Eng.* **2019**, *7*, 1059−1074.

(3) Shu, L.; Fan, Y.; Yang, Y.; Song, X.; Guo, H. Experimental study of shock pressure and erosion characteristics of high-pressure gas-liquid two-phase jet: Exploration for improving coalbed methane extraction efficiency. *Energy Sci. Eng.* **2023**, *11*, 1886−1905.

(4) Zuo, S.; Peng, S.; Zhou, D.; Wang, C.; Zhang, L. An analytical model of the initiation pressure for multilayer tree-type hydraulic fracturing in gas-bearing coal seams. *Geomech. Geophys. Geo.* **2022**, *8*, 206.

(5) Yang, R.; Zhang, H.; Zhang, J.; Wang, F.; Li, M.; Yin, T.; Wen, S.; Han, Y. Effects of Nanopore Structure Heterogeneity of Coal Samples on Adsorption Ability and Porosity-Permeability Variation. *Energy Fuels* **2023**, *37*, 2721−2734.

(6) Zuo, S.; Zhang, L.; Deng, K. Experimental study on gas adsorption and drainage of gas-bearing coal subjected to tree-type hydraulic fracturing. *Energy Rep.* **2022**, *8*, 649−660.

(7) Chen, S.; Tang, D.; Tao, S.; Liu, P.; Mathews, J. P. Implications of the in situ stress distribution for coalbed methane zonation and hydraulic fracturing in multiple seams, western Guizhou, China. *J. Pet. Sci. Eng.* **2021**, *204*, No. 108755.

(8) Wang, Y.; Bao, Y.; Hu, Y. Recent progress in improving the yield of microbially enhanced coalbed methane production. *Energy Rep.* **2023**, *9*, 2810−2819.

(9) Wang, C.; Zhang, C.; Li, Z.; Zhou, J. Using discrete element numerical simulation to determine effect of persistent fracture morphology on permeability stress sensitivity. *Int. J. Numer. Anal. Methods Geomech.* **2023**, *47*, 570−584.

(10) Ge, Z.; Shangguan, J.; Zhou, Z.; Li, Z.; Liu, L.; Chen, C.; Shao, C. Investigation of Fracture Damage and Breaking Energy Consumption of Hard Rock Repeatedly Cut by Abrasive Water Jet. *Rock Mech. Rock Eng.* **2023**, *56*, 3215−3230.

(11) Yang, F.; Ge, Z.; Zheng, J.; Tian, Z. Viscoelastic surfactant fracturing fluid for underground hydraulic fracturing in soft coal seams. *J. Pet. Sci. Eng.* **2018**, *169*, 646−653.

(12) Pan, L.; Zhang, S.; Zhang, J.; Lin, X. An experimental study on screening of dispersants for the coalbed methane stimulation. *Int. J. Oil Gas Coal Technol.* **2015**, *9*, 437−454.

(13) Ju, S.; Huang, Q.; Wang, G.; Li, J.; Wang, E. M.; Qin, C.; Qiao, J. Rheological and morphological characteristics of foam fluid using hydroxypropyl guar and surfactant. *J. Pet.Sci. Eng.* **2022**, *211*, No. 110124.

(14) Xu, T.; Mao, J.; Zhang, Q.; Lin, C.; Yang, X.; Zhang, Y.; Du, A.; Cun, M.; Huang, Z.; Wang, Q. Synergistic polymer fracturing fluid for coal seam fracturing. *Colloids Surf., A* **2021**, *631*, No. 127648.

(15) Wang, G.; Wang, Q.; Li, H.; Yan, S.; Huang, T.; Liu, X. Experimental study on the optimized anion fracturing fluid for improving coal samples permeability. *Energy Source, Part A* **2021**, 1−15.
(16) Wang, G.; Huang, T.; Yan, S.; Liu, X. Experimental study of the fracturing-wetting effect of VES fracturing fluid for the coal seam water injection. *J. Mol. Liq.* **2019**, *295*, No. 111715.
(17) Wang, C.; Zhou, G.; Jiang, W.; Niu, C.; Xue, Y. Preparation and performance analysis of bisamido-based cationic surfactant fracturing fluid for coal seam water injection. *J. Mol. Liq.* **2021**, *332*, No. 115806.
(18) Li, X.; Kang, Y.; Chen, D. Effect of Fracturing Fluid on Coalbed-Methane Desorption, Diffusion, and Seepage in the Ningwu Basin of China. *SPE Prod. Oper.* **2017**, *32*, 177−185.
(19) Yang, J.; Lian, H.; Li, L. Fracturing in coals with different fluids: an experimental comparison between water, liquid CO_2, and supercritical CO_2. *Sci. Rep.* **2020**, *10*, 18681.
(20) Lu, Y.; Yang, M.; Ge, Z.; Zhou, Z.; Chai, C.; Zhao, H. Influence of viscoelastic surfactant fracturing fluid on coal pore structure under different geothermal gradients. *J. Taiwan Inst. Chem. Eng.* **2019**, *97*, 207−215.
(21) Zuo, W.; Zhang, W.; Liu, Y.; Han, H.; Huang, C.; Jiang, W.; Mitri, H. Pore Structure Characteristics and Adsorption and Desorption Capacity of Coal Rock after Exposure to Clean Fracturing Fluid. *ACS Omega* **2022**, *7*, 21407−21417.
(22) Xue, S.; Huang, Q.; Wang, G.; Bing, W.; Li, J. Experimental study of the influence of water-based fracturing fluids on the pore structure of coal. *J. Nat. Gas Sci. Eng.* **2021**, *88*, No. 103863.
(23) Huang, Q.; Liu, S.; Wu, B.; Wang, G.; Li, G.; Guo, Z. Role of VES-based fracturing fluid on gas sorption and diffusion of coal: An experimental study of Illinois basin coal. *Process Saf. Environ. Prot.* **2021**, *148*, 1243−1253.
(24) Zhou, G.; Wang, C.; Wang, Q.; Xu, Y.; Xing, Z.; Zhang, B.; Xu, C. Experimental study and analysis on physicochemical properties of coal treated with clean fracturing fluid for coal seam water injection. *J. Ind. Eng. Chem.* **2022**, *108*, 356−365.
(25) Huang, Q.; Liu, S.; Wang, G.; Wu, B.; Yang, Y.; Liu, Y. Gas sorption and diffusion damages by guar-based fracturing fluid for CBM reservoirs. *Fuel* **2019**, *251*, 30−44.
(26) Yang, M.; Lu, Y.; Ge, Z. L.; Zhou, Z.; Chai, C.; Wang, H.; Zhang, L.; Bo, T. Viscoelastic surfactant fracturing fluids for use in coal seams: Effects of surfactant composition and formulation. *Chem. Eng. Sci.* **2020**, *215*, No. 115370.
(27) Bratcher, J. C.; Kaszuba, J. P.; Herz-Thyhsen, R. J.; Dewey, J. C. Ionic Strength and pH Effects on Water-Rock Interaction in an Unconventional Siliceous Reservoir: On the Use of Formation Water in Hydraulic Fracturing. *Energy Fuels* **2021**, *35*, 18414−18429.
(28) Qin, L.; Wang, P.; Lin, H.; Li, S.; Zhou, B.; Bai, Y.; Yan, D.; Ma, C. Quantitative characterization of the pore volume fractal dimensions for three kinds of liquid nitrogen frozen coal and its enlightenment to coalbed methane exploitation. *Energy* **2023**, *263*, No. 125741.
(29) Zuo, S.; Wang, C.; Liao, Y.; Peng, S.; Ma, Z.; Zhang, L. Mechanism of a novel ultrasonic promoting fracturing technology in stimulating permeability and gas extraction. *Energy Rep.* **2022**, *8*, 12776−12786.
(30) Ge, Z.; Wang, Z.; Hu, J.; Wang, Y.; Zhou, Z.; Li, R. Effect of different types of fracturing fluid on the microstructure of anthracite: an experimental study. *Energy Sources, Part A* **2021**, 1−15.
(31) Zheng, Y.; Zhai, C.; Chen, A.; Yu, X.; Xu, J.; Sun, Y.; Cong, Y.; Tang, W.; Zhu, X.; Li, Y. Microstructure evolution of bituminite and anthracite modified by different fracturing fluids. *Energy* **2023**, *263*, No. 125732.

https://doi.org/10.1021/acsomega.3c04351
ACS Omega 2023, 8, 29803−29811